Structural Macroeconometrics
Final Project

Dario Alfredo De Falco 0001078926
Francesco Di Marzio 0001084497

December 2023

Abstract

This paper investigates the effect of extreme climate shocks on the Italian macroeconomy in the last decades. We employ the indexes of severe events computed by IFAB[1], which measure anomalies in droughts, heat and cold stress, precipitation and wind. We build an extreme climate index by computing the first principal component of said indexes. We identify climate shocks by using an external instrumental variable, and we find unfavourable climate events to increase interest rates and decrease both GDP and gas prices. The effect on inflation is marginally significant.

1 Introduction

Climate change stands out as one of the most pressing challenges facing contemporary society, significantly altering our daily lives. Its far-reaching consequences touch multiple facets, ranging from increasingly unpredictable weather patterns to pervasive pollution in both water and land ecosystems. The urgency to address these issues has given rise to a nascent field of study that focuses on unraveling the intricate connections between extreme climate conditions and the economic apparatus.

While there is near-consensus on the link between climate and the macroeconomy in European countries, the specific mechanisms at play continue to be a topic of ongoing debate. Nonetheless, delving into the economic repercussions of climate shocks serves as the foundational step in shaping informed policy decisions, recognizing that a thorough understanding of these connections is vital for crafting effective strategies.

This research project makes a valuable contribution by presenting empirical evidence on the impact of climate shocks on key macroeconomic variables. With a specific focus on the Italian peninsula, the methodology involves constructing an index that encapsulates climate risk and combining it with data on inflation, GDP, and short-term interest rates in Italy. The comprehensive approach employs a Structural Vector Autoregression (SVARs) model, while the structural shocks are identified by means of a climate index measured in another country (Croatia) as an instrumental variable. The subsequent use of bootstrap inference aids in establishing confidence intervals for the estimates, lending significance or not to our findings.

Our results suggest an upward pressure on interest rates and contractionary effects on Gross Domestic Product and gas prices. The impact on inflation, however, remains marginal and inconclusive. These findings align with the notion that climate shocks act as adverse external forces on the economy, potentially leading to recession, and reinforcing the urgency of addressing climate-related challenges.

The research project unfolds across six paragraphs. Section 2 encompasses an overview of the existing literature, in section 3 we provide a detailed exploration of the employed data and the transformations we applied on it. In section 4 an in-depth discussion of the adopted econometric approach is presented. Section 5 contains an analysis

[1] IFAB stands for International Foundation Big Data and Artificial Intelligence for Human Development

of the obtained results for all methods. Finally, section 6 comprises of some indications for further research and improvements as well as some concluding remarks.

2 Literature review

Our research builds upon a recently emerging body of literature, with our starting point rooted in the analysis presented in a Master's thesis by Gjinaj [2023]. The author employs a Cholesky-SVAR model with the the European Extreme Events Climate Index (provided by IFAB) and several macroeconomic measures for Italy. Her findings indicate that unfavorable climate shocks increase inflation and reduce industrial production growth, while the effects on short-term interest rates and uncertainty indicators are negligible.

In contrast to this analysis, we adopt a more sophisticated approach to construct the climate index, employing principal component analysis. Additionally, several papers, such as Mukherjee and Ouattara [2021] and Kim et al. [2021], estimate the impact of climate shocks using Cholesky decomposition. We choose a proxy-SVAR identification scheme to leverage as much information as possible under the appropriate assumptions.

The use of proxies was pioneered by Stock and Watson [2008] and expanded by Stock and Watson [2012] and Mertens and Ravn [2013]. The latter paper contributes to the literature of estimating fiscal multipliers by using proxies to identify policy shocks. To estimate the uncertainty around our results, we employ a residual-based Moving Block Bootstrap (MBB). This bootstrap algorithm was initially proposed by Kunsch [1989] as an extension of the jackknife algorithm for estimating standard errors. Besides, Jentsch and Lunsford [2016] prove that wild bootstrap algorithm is invalid in our setup, whereas MBB preserves consistency. That said, we rely on these findings and use MBB in our analysis. Drawing inspiration from Ciccarelli et al. [2023], we isolate inflation related to food and energy from overall inflation to highlight the mechanism channel of climate shocks.

Moreover, the paper by Beirne et al. [2022], focusing on the Italian case and using the Emergency Events Database (EM-DAT), suggests upward inflationary pressures which are not found in our analysis. To enhance the robustness of our estimates against potentially weak instruments, we employ the novel Local Projection technique, guided by Fanelli and Marsi [2022] and Zivot et al. [1998].

3 Dataset

Our study utilizes a comprehensive dataset of monthly Italian macroeconomic and climatic data, covering the period from January 1997 to June 2023. Inflation is taken into account using two specific indices: the Harmonised Index of Consumer Prices (HICP) overall index, excluding food and energy, sourced from Eurostat, and the HICP specifically for food and energy, obtained from the European Central Bank (ECB). To prepare these series for analysis, we initially remove seasonality and trend components, followed by transforming the data through logarithms and calculating year-on-year growth rates by differencing with the same period in the previous year. To assess macroeconomic performance, we use a GDP index, which is seasonally adjusted and acquired from the Federal Reserve Economic Data (FRED) website, though originally compiled by the OECD. The interest rate we employ is the 3-month Italian inter-bank rate, with first differences taken to ensure stationarity. Lastly, our study includes data on net of tax heating gas prices, obtained from the Italian Ministry of Environment and Energy Security.This series is particularly relevant given the predominant role of gas in Italy's heating sector, as evidenced by sources such as ISTAT[2]. Notably, heating gas prices show a low correlation with general inflation but a higher correlation with food and energy inflation. This last feature actually will prove useful later, given that we fail to get significant result for food and energy inflation.

[2]See for example Ansa citing ISTAT

Our climatic series are provided by IFAB and Each series contains, for each month the number of standardized anomalies. Seasonality is taken into account as the exceedence is computed as the number of days in which some threshold percentile is surpassed of that month[3].

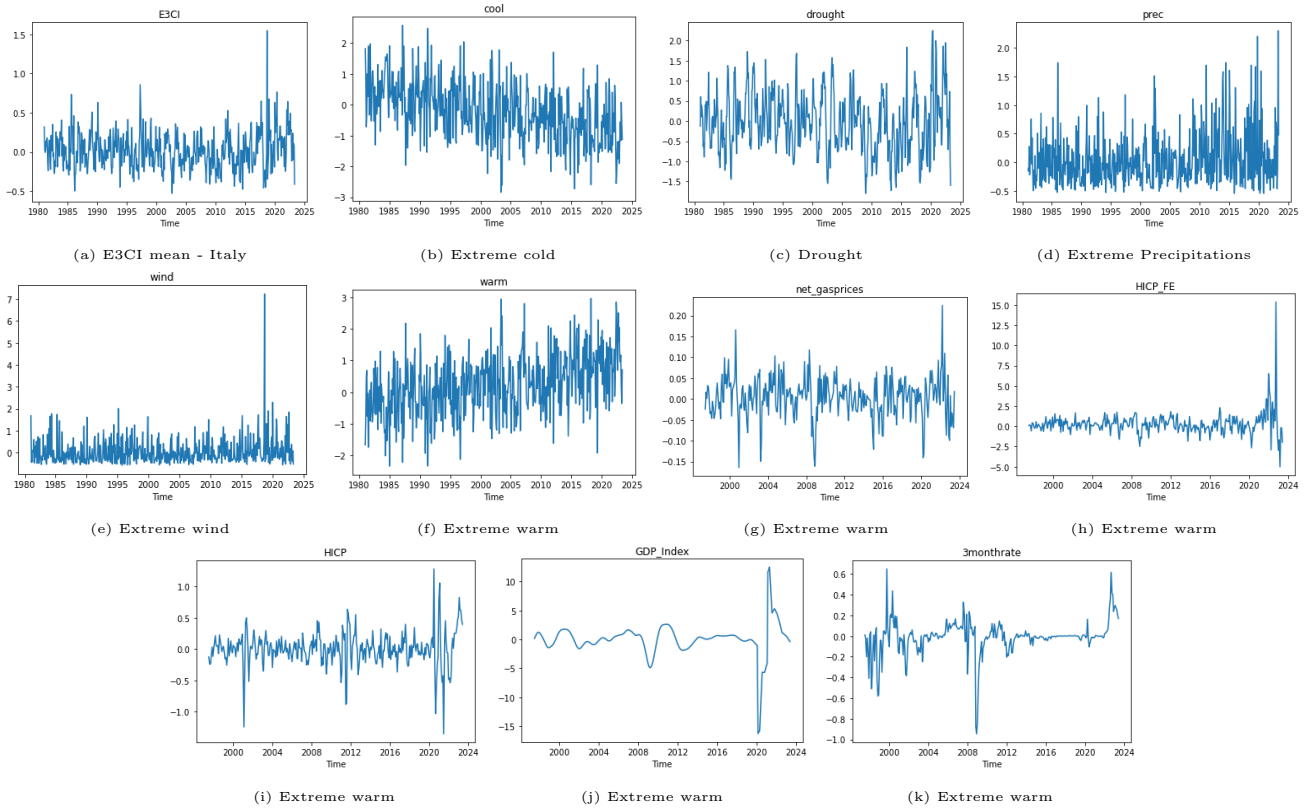

(a) E3CI mean - Italy (b) Extreme cold (c) Drought (d) Extreme Precipitations

(e) Extreme wind (f) Extreme warm (g) Extreme warm (h) Extreme warm

(i) Extreme warm (j) Extreme warm (k) Extreme warm

Figure 1: Climate and macroeconoomic series

[3]We first considered employing news based indicator for both macroeconomic and energy uncertainty. However, we found these series to be largely uncorrelated with the E3CI computed with the PCA. Therefore, we decided to concentrate on other variables, as we found non significant preliminary estimates.

4 Methodology

In this section, lowercase letters denote scalars, bold lowercase letters denote vectors, and uppercase letters denote matrices. To begin, we compute the first principal component using climate variables. We define the following column vector:

$$\mathbf{x}_t := (WARM_t, COLD_t, WIND_t, PREC_t, DROUGHT_t)'$$

Principal component analysis considers the variance-covariance matrix of these variables, defined as $\Sigma_X = \frac{1}{T}\sum_{t=1}^{T} \mathbf{x}_t \mathbf{x}_t'$. The largest eigenvalue of this matrix is 1.68, and the first principal component explains 60 percent of the total variance as shown in Figure 4. We denote the correspondent eigenvector as $\mathbf{v}$. The first principal component is computed as $E3CI_t = \mathbf{x}_t'\mathbf{v}$. The correspondent loadings are shown in Table 3. With the estimated climate index we then estimate a VAR model with the macroeconomic variables. We assume these variables fully describe the macroeconomy, and there are no confounding factors.

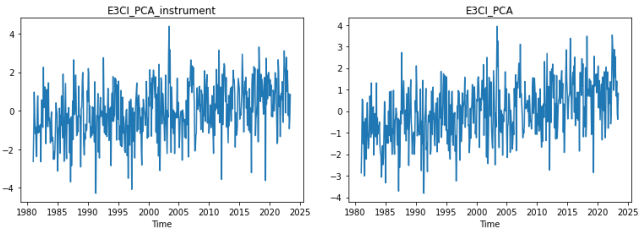

(a) E3CI PCA - Croatia (b) E3CI PCA - Italy

Figure 2: Climate stress indicator, computed using PCA

After evaluating criteria such as the Akaike Information Criterion (AIC), Bayesian Information Criterion (BIC), Hannan-Quinn Criterion (HQC), and the likelihood ratio test (as detailed in Table 1), the suggestion was to employ a single lag. However, these tests often demonstrate unreliability in small sample sizes. Consequently, we opted for a two-lag approach, hypothesizing that the initial assessment might overlook certain autoregressive characteristics in the data. Employing two lags allows for a more nuanced capture of the data's dynamic behavior. Additionally, the augmented Dickey-Fuller test was applied to all variables, including the instrumental variable. Results, displayed in Table 2, confirm stationarity at the 1% significance level for all variables. VAR innovations are assumed to follow a Gaussian distribution. Recognizing the correlation among VAR innovations, we transition to a structural model. Structural shocks are denoted as $\boldsymbol{\varepsilon}_t$, satisfying $E(\boldsymbol{\varepsilon}_t) = \mathbf{0}$ and $V(\boldsymbol{\varepsilon}_t) = I$. We link innovations and structural shocks through a matrix K. Overall, we consider the following model specification:

$$\begin{cases} \mathbf{w}_t := (E3CI_t, GASPR_t, HICP_{FE_t}, HICP_t, GDP_t, IRATE_t)' \\ \mathbf{w}_t = \boldsymbol{\mu} + \boldsymbol{\gamma} t + A_1 \mathbf{w}_{t-1} + A_2 \mathbf{w}_{t-2} + \mathbf{u}_t \\ \mathbf{u}_t \sim \mathcal{N}(\mathbf{0}, \Sigma_u) \\ \mathbf{u}_t = K \boldsymbol{\varepsilon}_t \end{cases}$$

The VAR model is estimated using maximum likelihood estimation, where the likelihood function takes the form:

$$\mathscr{L}(\bullet) = (2\pi)^{-\frac{kT}{2}} |\Sigma_u|^{-\frac{T}{2}} \exp\left\{ -\frac{1}{2} \sum_{t=1}^{T} \mathbf{u}_t' \Sigma_u^{-1} \mathbf{u}_t \right\}$$

We now consider the generic structural Impulse Response Function:

$$IRF_{\bullet,\bullet}(h) = RJ^h R' K$$

In this analysis, our focus lies on the impact of the climate index. We define $\boldsymbol{\kappa}$ as the on-impact coefficients of this variable (i.e., the first column of matrix K). Our target IRF is expressed as:

$$IRF_{\bullet,1}(h) := \boldsymbol{\phi}_h = RJ^hR'\boldsymbol{\kappa}$$

By the Continuous Mapping Theorem, we require consistent estimators of both J and $\boldsymbol{\kappa}$ to achieve a consistent estimate of the target IRF. The estimate of the companion matrix $\hat{J}$ is derived as:

$$\hat{J} = \begin{pmatrix} \hat{A}_1 & \hat{A}_2 \\ I & O \end{pmatrix}$$

where I denotes the identity matrix and O denotes matrix of zeros. The variance-covariance matrix of the residuals is defined as $\hat{\Sigma}_u = \frac{1}{T-p}\sum_{t=p+1}^{T} \hat{\mathbf{u}}_t\hat{\mathbf{u}}_t'$. Next, we introduce the instrumental variable, E3CI of Croatia, denoted as z_t. We assume that the instrumental variable is both relevant (correlated with the target structural shock) and exogenous (uncorrelated with non-target structural shocks). This is summarized as:

$$\begin{cases} \varrho := E(z_t\varepsilon_{1t}) > 0 \\ E(z_t\varepsilon_{jt}) = 0, \quad \forall j = 2,3,4,5,6 \end{cases} \tag{1}$$

Since $V(\varepsilon_{1t}) = 1$ by definition, the validity condition can be expressed as follows:

$$\begin{cases} z_t = \varrho \cdot \varepsilon_{1t} + 0 \cdot \varepsilon_{2t} + ... + 0 \cdot \varepsilon_{8t} + \upsilon_t \\ \upsilon_t \sim \text{MDS} \end{cases} \tag{2}$$

The covariance between the instrument and VAR innovations is given by $E(\mathbf{u}_t z_t) := \boldsymbol{\varphi}$. A consistent estimator is $\hat{\boldsymbol{\varphi}} = \frac{1}{T-p}\sum_{t=p+1}^{T} \hat{\mathbf{u}}_t z_t$. The following equation holds: $\boldsymbol{\varphi} = \varrho\boldsymbol{\kappa}$. We then introduce another moment condition to distinguish between the two components. Indeed, it can be shown that $\boldsymbol{\varphi}'\Sigma_u^{-1}\boldsymbol{\varphi} = \varrho^2$. Overall, we compute:

$$\hat{\boldsymbol{\kappa}} = \left\{\hat{\boldsymbol{\varphi}}'\hat{\Sigma}_u^{-1}\hat{\boldsymbol{\varphi}}\right\}^{-\frac{1}{2}}\hat{\boldsymbol{\varphi}}$$

This is proven to be consistent for the on-impact coefficient $\boldsymbol{\kappa}$. The asymptotic variance covariance matrix can be estimated consistently by using a Classical Minimum Distance approach (Angelini and Fanelli [2019]). As previously stated, we eventually achieve a consistent estimator of the target IRF, that is $\hat{\boldsymbol{\phi}}_h = R\hat{J}^hR'\hat{\boldsymbol{\kappa}}$.

4.1 Instrument

We choose to employ the E3CI index computed with PCA for Croatia as an instrument. We deem this instrument to be relevant as it is highly correlated with the shock of interest ε_{1t}, with a correlation always greater than 0.82 and varying mildly between different VAR specifications[4]. Intuitively, this makes sense as Italy and Croatia are both in the Mediterranean area and the coast of Croatia lies entirely on the Adriatic sea, which also touches upon Italy's beaches. The correlation coefficient is computed as $\rho = \frac{(\hat{\boldsymbol{\psi}}'\hat{\Sigma}_u^{-1}\hat{\boldsymbol{\psi}})^{\frac{1}{2}}}{\sigma_z}$. Where σ_z denotes the standard deviation of the instrumental variable. Our choice of the instrument is justified also by its exogeneity. Given that Croatia is a small country, we can assume that the instrument is not causally linked to the Italian macroeconomic variables. In other words, we assume that a climate shock to the Croatian economy is not relevant for the Italian one because Croatia is a small economy. Thus, given that the instrument is relevant and exogenous we assume conditions 1 and 2 to hold. These facts imply that a climate shock in Croatia is related to Italian macroeconomic variables only through the E3CI for Italy itself.

[4]We didn't provide a table showcasing these correlations, as they do not vary by much. However, the code directly replicates this.

4.2 Bootstrap confidence bands

In order to compute the confidence intervals we employ an overlapping Moving Block Bootstrap (MBB), following the methodology described in Jentsch and Lunsford [2022]. This methodology allows us to recreate the sample while keeping the autoregressive nature of our series. We are not concerned about the fact that the observation in the first and last few blocks have a slightly lower probability of being chosen. This is because our chosen block length is only 12. We define T as the total number of observations, M as the number of variables and l as the length of the block. The procedure for each bootstrap iteration is outlined below:

1. We build $T-p-l+1$ overlapping blocks containing the instrument and the residuals for each time period[5], and we randomly sample from these blocks without replacement to reconstruct a time series of the residuals. Whenever a block is chosen, it is also re-centered by subtracting the mean of the block itself. We extract $\frac{T-p}{l}+1$ observations and then keep only $T-p$ of them. This procedure allows to choose any block length, even if it's not a divisor of the effective sample, $T-p$.

2. Once we have the bootstrap residuals, we construct the bootstrap sample according to the following scheme:

$$\begin{cases} \mathbf{w}_1^* = \mathbf{w}_1 \\ \mathbf{w}_2 = \mathbf{w}_2 \\ \mathbf{w}_3^* = \boldsymbol{\mu} + 3\boldsymbol{\gamma} + A_1\mathbf{w}_2^* + A_2\mathbf{w}_1^* + \mathbf{u}_3^* \\ \mathbf{w}_4^* = \boldsymbol{\mu} + 4\boldsymbol{\gamma} + A_1\mathbf{w}_3^* + A_2\mathbf{w}_2^* + \mathbf{u}_4^* \\ \vdots \\ \mathbf{w}_T^* = \hat{\boldsymbol{\mu}} + T\hat{\boldsymbol{\gamma}} + + A_1\mathbf{w}_{T-1}^* + A_2\mathbf{w}_{T-2}^* + \mathbf{u}_T^* \end{cases}$$

3. Compute the bootstrap estimates of the companion matrix and the bootstrap variance covariance matrix of residuals in order to get $\hat{J}^*$ and $\hat{\Sigma}_u^*$. Compute the bootstrap version of $\boldsymbol{\varphi}^*$ and get the bootstrap on-impact coefficients as $\hat{\boldsymbol{\kappa}}^* = \left\{\hat{\boldsymbol{\varphi}}^{*\prime}\hat{\Sigma}_u^{*-1}\hat{\boldsymbol{\varphi}}^*\right\}^{-\frac{1}{2}}\hat{\boldsymbol{\varphi}}^*$.

4. Compute the bootstrap IRF as $\hat{IRF}^*_{\bullet,1}(h) := \hat{\boldsymbol{\phi}}_h^* = R\hat{J}^{*h}R'\hat{\boldsymbol{\kappa}}^*$.

These four steps are repeated $B = 20000$ times for each model that employs the bootstrap. We find that with this number of iterations it is not necessary to set a random seed to obtain the same confidence bands across replications of the results. This seems a correct procedure as the bootstrap convergence and validity shouldn't rest upon a random seed fixing the pseudo-random number generator that selects blocks and thus influences the results. The confidence bands are extracted from the bootstrap in that for each horizon and variable we take the top and bottom quantiles across bootstrap replications. More formally, we know by Glivenko Cantelli that for a large enough number of bootstrap iterations B, the quantiles estimated with the bootstrap procedure converge almost surely to the bootstrap quantiles q^*_{i1h}:

$$\hat{q}^*_{i1h;B} \xrightarrow{a.s.} q^*_{i1h}, \quad B \to \infty$$

Therefore by assuming bootstrap consistency, the bootstrap quantiles converge in probability to the quantiles of the distribution of $\hat{\boldsymbol{\kappa}}$:

$$q^*_{i1h} \xrightarrow{p} q_{i1h}, \quad T \to \infty$$

Given our methodology, we assume that we have a sufficiently large sample, and run a sufficiently large number of iterations for these two results to hold. This guarantees that we can make inference based on the bootstrap

[5] Which amounts to 299 block in our case, for $T = 312$, $p = 2$, and $l = 12$

quantiles.

4.3 Local Projections

To extend our analysis to the case of weak instrument we employ local projections in the wake of Fanelli and Marsi [2022] and Zivot et al. [1998]. This approach robustifies inference to the presence of weak instruments by computing Anderson and Rubin (AR) identification-robust confidence sets for the parameters of interest. That is, the impact of the climate shock on each variable for each horizon. Following Fanelli and Marsi [2022], the estimated local projections are given, for horizon $h = 0, 1, ..., 24$ and variable $i = 1, ..., 6$ by the equations below:

$$Y_{i,t+h} = \mu_{i,h} + \delta_{i,h}t + \beta_{i,h}E3CI_t + \sum_{l=1}^{2} A'_{i,l,h}Y_{t-l} + \sum_{l=1}^{2} \rho_{i,l,h}z_{t-l} + \eta_{i,t+h} \tag{3}$$

where $\mu_{i,h}$ represents the constants and $\delta_{i,h}$ the coefficients for the time trend, $\eta_{i,t+h}$ are the projection errors, $\beta_{i,h}$ are the estimated responses of the dependent variables to a shock at time t in the $E3CI_t$. Under $H_0 : \beta_{i,h} = \beta^0_{i,h}$ we rewrite 3 as :

$$Y_{i,t+h} - \beta^0_{i,h}E3CI_t = \mu_{i,h} + \delta_{i,h}t + (\beta_{i,h} - \beta^0_{i,h})E3CI_t + \sum_{l=1}^{2} A'_{i,l,h}Y_{t-l} + \sum_{l=1}^{2} \rho_{i,l,h}z_{t-l} + \eta_{i,t+h} \tag{4}$$

Furthermore, we define the first stage regression as:

$$E3CI_t = \rho Z_t + \sum_{l=1}^{2} A'_{i,l,h}Y_{t-l} + \sum_{l=1}^{2} \rho_{i,l,h}z_{t-l} + v_t \tag{5}$$

Therefore by substituting 5 in 4, we obtain the following:

$$g_{i,t+h} = \mu_{i,h} + \delta_{i,h}t + \zeta^0_i z_t + \sum_{l=1}^{2} A'_{i,l,h}Y_{t-l} + \sum_{l=1}^{2} \rho_{i,l,h}z_{t-l} + \eta_{i,t+h}*$$

Where $g_{i,t+h} = Y_{i,t+h} - \beta^0_{i,h}E3CI_t$, $h = 0, 1, ..., 24$, $\zeta^0_i = (\beta_{i,h} - \beta^0_{i,h})\rho$, $\eta_{i,t+h}* = \eta_{i,t+h} + (\beta_{i,h} - \beta^0_{i,h})v_t$. We choose $\beta^0_{i,h}$ by iterating over a grid ranging from -1 to 1.2 with incremental steps of 0.001. For each value in the grid, each horizon and variable we compute a t-test for the null hypothesis that $\zeta^0_i = 0$, we consider all the values for which this hypothesis is not rejected, thereby composing the confidence set. The estimate with the highest p-value for each horizon and variable is chosen as the point estimate.

4.4 Programming Language

The software implementation is done in Python, although we seldom use a Python api that allows to exploit matlab as the computation engine[6]. Both the code and the dataset can be found on GitHub. Overall, the code runs pretty smoothly, with the most intensive computations being the ones related to the Bootstrap. With the standard NumPy computations, the bootstrap takes 150 seconds to complete with 20 thousands iterations, whilst only 90 seconds are needed if a parallel computing implementation is used. Both approaches are already implemented in the code, but the former is the most widely compatible and puts less stress on the computer. The code allows for both options, with the first being the most widely compatible. At the end of the code also an embryonic version of the Local Projection is present. Unfortunately, we are not able to complete it and include it in the present paper.

[6]Indeed, we use matlab to check the robustness of our VAR computation scheme. For all VAR models, the results using Matlab "estimate" function and the ones found with our code are the same.

5 Empirical results

As shown in Figure 9, the eigenvalues of the estimated companion matrix lie within the unit circle, indicating stability. The estimates of the Impulse Response Functions (IRFs) are presented in Figure 3. Overall, the analysis reveals that the point estimates of all IRFs exhibit stationary behavior. This is highlighted by their tendency to gradually converge towards zero without changing sign as the time horizon extends. An exception to this pattern is observed in the IRF related to the Harmonised Index of Consumer Prices (HICP) excluding food and energy, which demonstrates a non-significant oscillation around zero. Bootstrap methods are employed to calculate the mean and construct confidence intervals at the 95%, 90%, and 68% levels. The analysis begins with the top left panel of the IRFs. Here, the immediate impact coefficient for the climate shock is approximately 1.2, which aligns with the standard deviation of the E3CI. This alignment suggests an accurate identification of the climate shock in the model. Moreover, the coefficient is significant and the confidence bands at all levels are noticeably narrow. Significance at all levels is lost at $h = 3$. The impact of a climate shock on the net price of gas is negative and significant at all levels. Significance is lost after 2 and 3 periods for the 95 and the 90 and 68 percent confidence levels. Surprisingly, the impact of a climate shock on the inflation related to unprocessed food and energy is not significant at all significance levels and all horizons. The IRF for the HICP excluding these items shows a significant positive coefficient on impact at all levels. Significance is lost at all levels for $h = 1$ but is restored for $h = 2$ and $h = 3$, albeit only at 90 and 68 confidence levels. The impact of a climate shock on GDP is negative and is only significant at the 68 percent level on impact. At $h = 1$ it becomes significant at the 90 percent level, and at $h = 2$ it becomes significant also at the 95 percent level, becoming non significant at this level afterwards. The effect remains significant and negative up until $h = 4$ at the 90 confidence interval and until $h = 7$ for the 68 percent interval. This is the response that lasts the longer. Finally, the effect on the 3 month inter-bank rate is positive but non significant on impact at all levels. It becomes significant for the 68 and 90 levels at $h = 1$ and remains so up until $h = 3$. At the 95 percent level, significance is achieved at $h = 1$ and $h = 2$, where the bands start including 0. As a final comment, our estimates do not differ much from the bootstrap mean, especially for the IRF related to the E3CI and for the 3 month interest rate. For these IRFs the bootstrap mean and the point estimate basically overlap. In the rest of the IRFs we see some discrepancy, albeit small, between these two quantities. This provides evidence towards a mild bias of our estimation technique, likely stemming from the small number of variables employed in the model. Bias correction could be possible but it's avoided since it is beyond the scope of this project.

5.1 Robustness check

We suspect that the correlation between unprocessed food and energy, as well as heating gas, might lead to inaccuracies in our inflation estimates. To address this, we constructed two VAR models: one excluding inflation related to unprocessed food and energy but including heating gas, as depicted in Figure 7, and another excluding heating gas but retaining unprocessed food and energy inflation, shown in Figure 8. The results from both models are strikingly similar, suggesting no significant differences in the estimates. Furthermore, we check what happens by directly using 'warm' as the climate variable, the series with the highest loading in our PCA. The associated Impulse Response Functions (IRFs) are depicted in Figure 5. These IRFs closely resemble those obtained using the full PCA, which is unsurprising given 'warm's dominant loading. This similarity underscores how extreme climate events, primarily manifested through temperature increases, can significantly affect our model. This finding is particularly relevant for data-scarce situations, indicating that a single series might suffice for reliable estimation. Our final analysis involved using the E3CI, calculated as the average of five underlying series, also applied to the instrumental variable. The results, presented in Figure 6, largely align with those obtained using the PCA, though with wider confidence intervals that consistently encompass zero for both heating gas prices and the three-month interbank rate. Notably, the IRF for inflation and unprocessed food is positive and significant at a 68% confidence level at h=1,but loses significance beyond that point. This observation suggests that different components of the

index may have distinct transmission mechanisms and macroeconomic effects. Consequently, employing various linear combinations of these series can yield different estimations, highlighting the need for careful selection and analysis of data series in econometric modeling.

5.2 Economic Interpretation

Considering our results, it's important to delve into and hypothesize about the potential mechanisms through which climate shocks can influence the macroeconomy. A key aspect of this discussion is the effect of climate shocks, particularly extreme temperature increases, on the price of heating gas. The leading component of our indicator, labeled 'extreme hot', likely plays a crucial role in this context. For instance, a sudden rise in temperature during winter months can logically lead to a decreased demand for heating gas. This relationship is particularly noteworthy given that our data has been seasonally adjusted. It's crucial to point out that even in the absence of direct seasonal adjustment, the process of logarithmic transformation and differencing of the data inherently addresses any seasonality concerns. Therefore, the observed impact of extreme temperature changes on heating gas demand and pricing appears to be independent of seasonal effects. This insight is vital for understanding the broader economic implications of climate variability, especially in sectors like energy, where demand is closely tied to weather patterns.

Our initial hypothesis posited that climate shocks would predominantly affect inflation through unprocessed food and energy prices. Contrary to this belief, our empirical findings suggest otherwise. This discrepancy could stem from the high volatility inherent in these prices and the potential omission of variables significantly correlated with them, highlighting a key limitation of our VAR model. Further refinements seem necessary to address these issues. Notably, the volatility of energy prices often overshadows fluctuations in food prices. Almost all the series' informational content appears to be encapsulated within energy prices, leading us to believe that disaggregating these series might yield more insightful analyses. Although we have verified this through manual checks, detailing these findings would excessively elongate this work. Additionally, separate inclusion of food and energy prices was hindered by data unavailability.

The estimated impact of climate shocks on inflation is positive and tends to persist for up to four or five periods, depending on the chosen confidence level. We conjecture that supply disruptions are the primary channel for this impact. For instance, heatwaves could trigger crop failures, thereby placing upward pressure on prices in the non-food sector. Similarly, natural disasters like floods can cause temporary or permanent shutdowns of local businesses. This effect is particularly pronounced in Italy, where the economy is heavily reliant on small businesses ill-equipped to withstand significant, unforeseen climate-related stresses. These dynamics also help explain the observed negative impact on GDP and the positive impact on the three-month interbank rate following climate shocks. The Italian banking sector, characterized by its small size, fragmentation, and lack of diversification, is particularly vulnerable. Many Italian banks are local and tend to lend predominantly to small local businesses. While this facilitates the accumulation of significant private information, it also results in poor diversification. As these businesses face stress from climate shocks, the banks lending to them come under pressure too. For a tangible example, consider the 2023 flood in Eastern Emilia Romagna, which caused substantial local supply disruptions, reflecting the Italian system's broad exposure to such events. The resultant increase in uncertainty and risk logically leads to higher interest rates.

In summary, the transmission mechanisms of climate shocks are likely highly specific to individual countries, and conducting cross-country analyses or investigations within smaller administrative regions could provide particularly valuable insights."

5.3 Local Projections Results

For a robustness check, we employ the local projection method using a strong instrument, with results presented in Figure 10[7]. Additionally, we estimate the Impulse Response Functions (IRFs) using local projection with a weak instrument, specifically the average global sea level. This variable is chosen due to its exogenous nature and strong link to global climate change, potentially serving as a proxy for Italian climate shocks. However, a significant limitation of this instrument is its slower pace relative to the extreme climate events included in our series. Consequently, we do not anticipate the resulting IRFs to be highly informative, even with the application of weak instrument robust inference methods. In fact, the estimated confidence intervals for the IRFs for each variable are very wide and lack significance, leading to their omission for brevity[8]. Future research may find more success using a different weak instrument.
Returning to our estimates using the strong instrument and local projection method, Figure 10 reveals that the results do not substantially differ from those obtained through proxy-SVAR estimates for the 6-variable model, as shown in 3. Both the direction of effects and the confidence intervals are generally similar, particularly in the initial periods. The main and most interesting difference is the presence of significant effects at horizon that are relatively far from 0. In fact, the IRFs estimated with Proxy-SVARs are never significant past $h = 10$ at any significance level. However, the IRF for the net price of gas shows significance at $h = 7, 21$ at the 90% confidence interval, and the same occurs also at other horizons past $h = 10$, albeit only at the 68% level. Something similar occurs also for the IRF related to there month interbank rate. The estimate is significant for many periods at the 68% level, and is significant at both confidence intervals also for horizons between 9 and 12, and at $h = 24$. The IRF estimate for GDP is significant only at the 68% level. Surprisingly the IRF for inflation related to unprocessed food and energy is negative and significant for $h = 7$ at both confidence intervals, and is significant for more periods but only at the 68%.

Overall, the local IRFs confidence set resulting from the Local projections method share the same sign as the proxy-SVAR estimates but show significantly more persistence. We are skeptical in claiming that this persistence is a feature of the data, we rather see this just as a statistical curiosity arising from the limited number of observations comprising our sample. Further research would be needed to properly shed light on the topic, allowing researchers to take a stance on it. What we can say is that the sign and early horizons significance we observed in our proxy-SVAR, is confirmed by the local projections.

6 Concluding remarks

6.1 Limitations and potential improvements

Our model model could be improved through the inclusion of more information in the VAR by creating appropriate factors. For example if one were interested in the effect of climate shocks on a few variables, one could employ in the VAR the climate shocks, the variables of interest and some controls constructed with factor analysis, in the wake of Bernanke et al. [2005]. This would make the VAR analysis more robust and comprehensive, limiting the impact of possibly omitted variables. To improve the estimates, the implementation of bias-corrected OLS estimators as suggested by Kilian [1998] could prove beneficial. However, this is not a main issue of concern, as shown by the IRFs the bias does not seem to be a large factor in our analysis. Although small, its presence is shown by the fact that the bootstrap mean estimate is not the same as our point estimate, around which it should be centered.

[7] Please note that the absence of a confidence interval for $E3CI_{PCA}, h = 0$ is by construction.
[8] This can be replicated by setting the "use_weak" dummy variable to 1 in the code

6.2 Conclusion

We find that climate shocks have a detrimental impact on the macroeconomy, characterized by increased interest rates and inflation alongside a reduction in GDP. Interestingly, these shocks appear to lower heating gas prices, which we hypothesize is due to decreased demand. Our results consistently show significance at the 95% or 90% confidence levels and are robust to weakness of the instrument. The exact mechanisms behind these effects remain unclear, suggesting a need for further theoretical exploration, potentially revealing country-specific dynamics. In the case of Italy, the unique economic structure predominantly composed of very small businesses and local banks may explain a large portion of the transmission mechanism of climate shocks on its macroeconomy. Further research could explore these dynamics in different country contexts to better understand the transmission mechanism at play. Moreover, employing single series instead of a linear combination of them seems to be a viable strategy, useful in data sparse environments.

References

Giovanni Angelini and Luca Fanelli. Exogenous uncertainty and the identification of structural vector autoregressions with external instruments. *Journal of Applied Econometrics*, 34(6):951–971, 2019.

John Beirne, Yannis Dafermos, Alexander Kriwoluzky, Nuobu Renzhi, Ulrich Volz, and Jana Wittich. Natural disasters and inflation in the euro area. 2022.

Ben S Bernanke, Jean Boivin, and Piotr Eliasz. Measuring the effects of monetary policy: a factor-augmented vector autoregressive (favar) approach. *The Quarterly journal of economics*, 120(1):387–422, 2005.

Matteo Ciccarelli, Friderike Kuik, and Catalina Martínez Hernández. The asymmetric effects of weather shocks on euro area inflation. 2023.

Luca Fanelli and Antonio Marsi. Sovereign spreads and unconventional monetary policy in the euro area: A tale of three shocks. *European Economic Review*, 150:104281, 2022.

Antonela Gjinaj. When climate turns extreme: Assessing the impact of climate shocks on the macroeconomy and uncertainty. *Master Thesis*, 2023.

Carsten Jentsch and Kurt G Lunsford. Proxy svars: asymptotic theory, bootstrap inference, and the effects of income tax changes in the united states. 2016.

Carsten Jentsch and Kurt G Lunsford. Asymptotically valid bootstrap inference for proxy svars. *Journal of Business & Economic Statistics*, 40(4):1876–1891, 2022.

Lutz Kilian. Small-sample confidence intervals for impulse response functions. *Review of economics and statistics*, 80(2):218–230, 1998.

Hee Soo Kim, Christian Matthes, and Toan Phan. Extreme weather and the macroeconomy. *Available at SSRN 3918533*, 2021.

Hans R Kunsch. The jackknife and the bootstrap for general stationary observations. *The annals of Statistics*, pages 1217–1241, 1989.

Karel Mertens and Morten O Ravn. The dynamic effects of personal and corporate income tax changes in the united states. *American economic review*, 103(4):1212–1247, 2013.

Krishnendu Mukherjee and Bakary Ouattara. Climate and monetary policy: do temperature shocks lead to inflationary pressures? *Climatic change*, 167(3-4):32, 2021.

James H. Stock and Mark W. Watson. Nber summer institute minicourse 2008: What's new in econometrics–time series, lecture 7: Structural vars. *Cambridge, Mas: National Institute for Economic Research*, 2008.

James H Stock and Mark W Watson. Disentangling the channels of the 2007-2009 recession. Technical report, National Bureau of Economic Research, 2012.

Eric Zivot, Richard Startz, and Charles R. Nelson. Valid confidence intervals and inference in the presence of weak instruments. *International Economic Review*, 39(4):1119–1144, 1998. ISSN 0020-6598. doi: 10.2307/2527355.

Tables and Figures

Lag	AIC	BIC	HQC	LogLikelihood	LR Test p-value
1	1535.298137*	1696.853999*	1589.096560*	-710.671969	1.970309e-02
2	1597.252097	1847.657503	1659.258225	-682.892715	8.768161e-02
3	1712.289396	2005.822265	1736.932947	-658.910656	4.122571e-03
4	1891.837853	2149.336068	1800.109181	-627.720251	9.080713e-08
5	2190.698809	2256.148313	1826.737001	-578.296773	1.060823e-07
6	2870.370016	2363.191576	1853.749663	-529.107086	NaN

Table 1: Criteria and LR test for 6 variables VAR

	$E3CI_{PCA_{IT}}$	$E3CI_{PCA_{CR}}$	$E3CI_{mean_{IT}}$	$E3CI_{mean_{CR}}$	$GASPR$	$HICP_{FE}$	$HICP$	GDP_{Index}	$IRATE$
ADF Statistic	-10.08	-14.31	-8.71	-11.07	-11.86	-4.14	-5.97	-4.71	-7.51
p-value	1.18e-17	1.18e-26	3.62e-14	4.42e-20	6.96e-22	0.82e-3	1.921e-07	8.03e-05	3.96e-11

Table 2: ADF Statistics and p-values for all the variables employed VARs

Country	Cool	Drought	Precipitation	Wind	Warm
Italy	-0.69374085	0.10349399	-0.05888825	-0.07114397	0.70674135
Croatia	-0.62147314	0.25808729	-0.22314799	-0.21649142	0.67119187

Table 3: First Principal component's loadings for Italy and Croatia

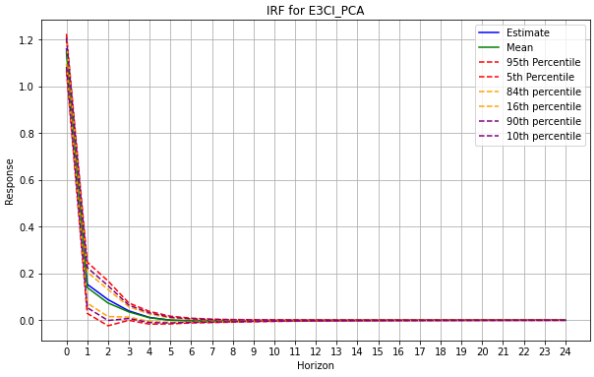

(a) E3CI PCA

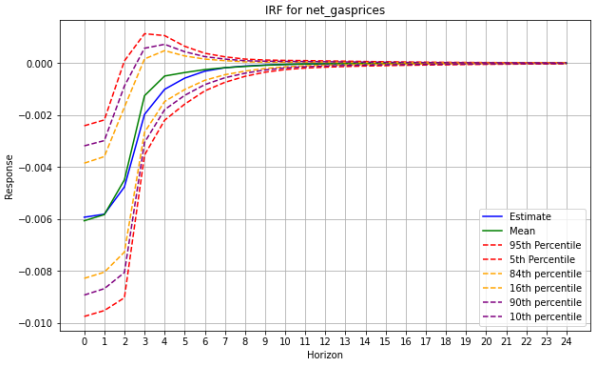

(b) Net price of heating gas

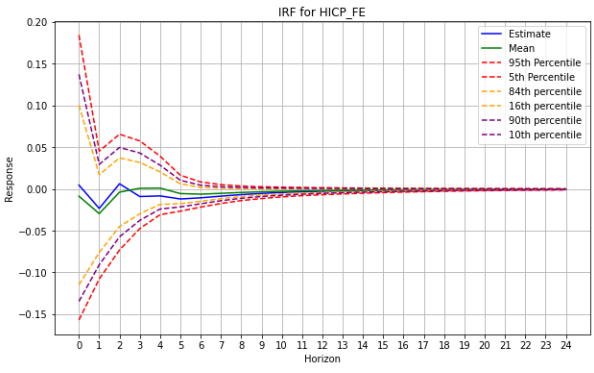

(c) HICP for food and energy

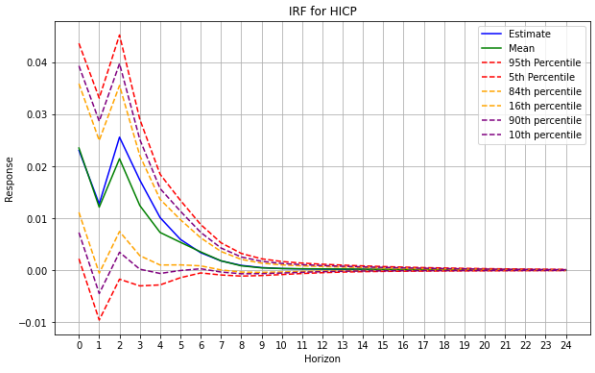

(d) HICP excluding food and energy

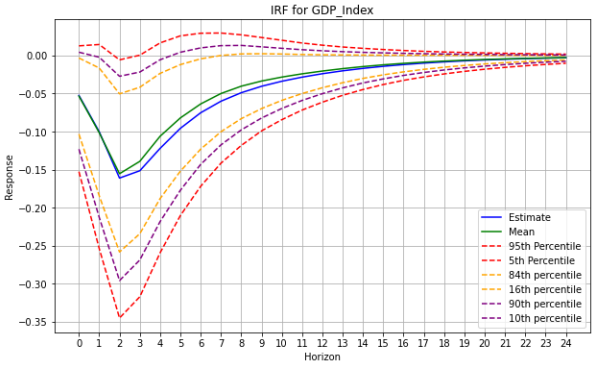

(e) GDP index

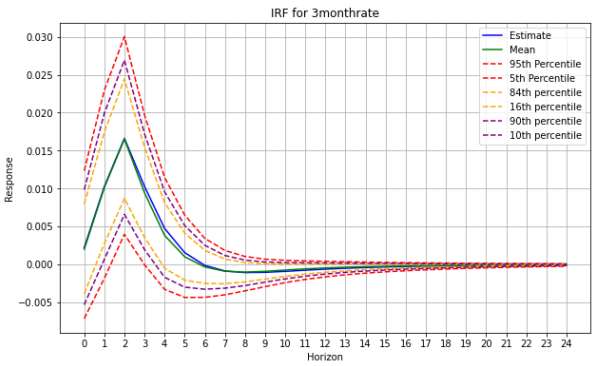

(f) Three month interbank rate

Figure 3: IRFs for 6 variables using E3CI PCA, 20000 bootstrap iterations

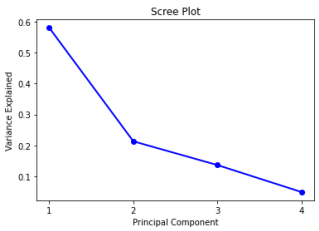

(a) Scree plot for the Italian E3CI

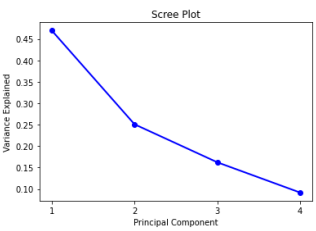

(b) Scree plot for the Croatian E3CI

Figure 4: Scree plot of Italian(left) and Croatian(Right) climate series

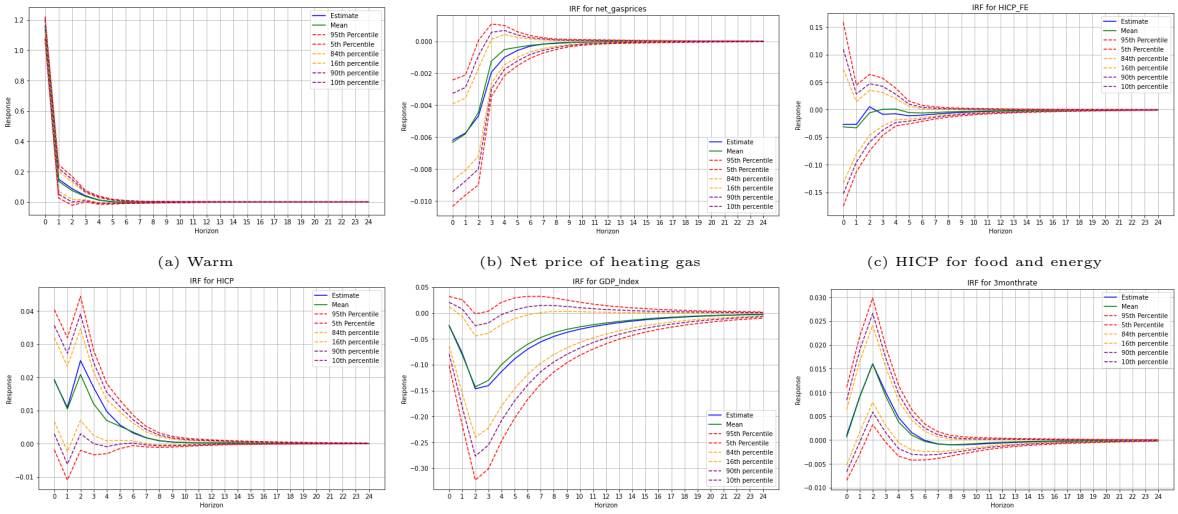

(a) Warm (b) Net price of heating gas (c) HICP for food and energy

(d) HICP excluding food and energy (e) GDP index (f) Three month interbank rate

Figure 5: IRFs for 6 variables using warm, 20000 bootstrap iterations

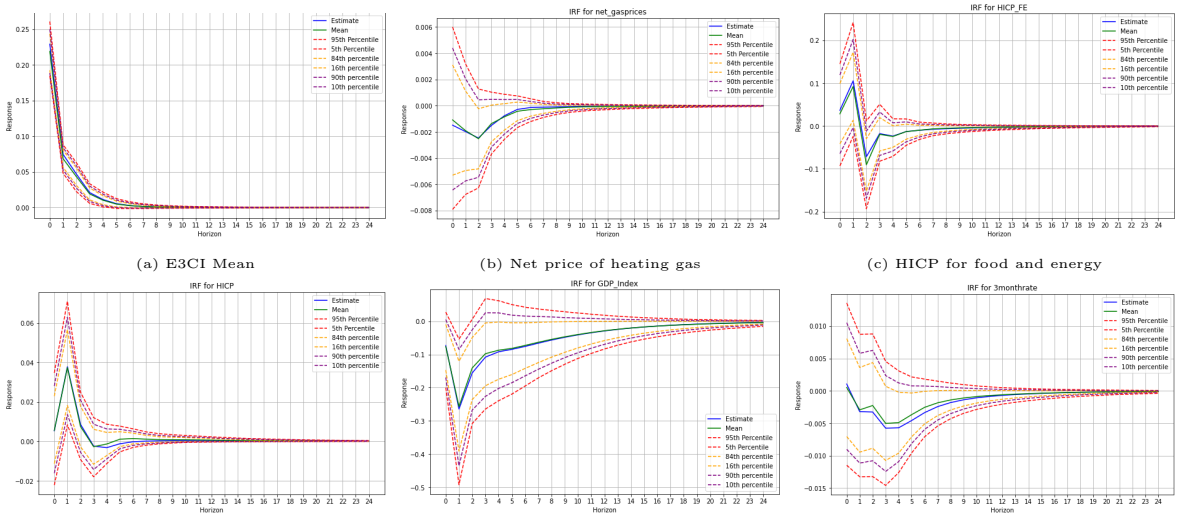

(a) E3CI Mean (b) Net price of heating gas (c) HICP for food and energy

(d) HICP excluding food and energy (e) GDP index (f) Three month interbank rate

Figure 6: IRFs for 6 variables using E3CI mean, 20000 bootstrap iterations

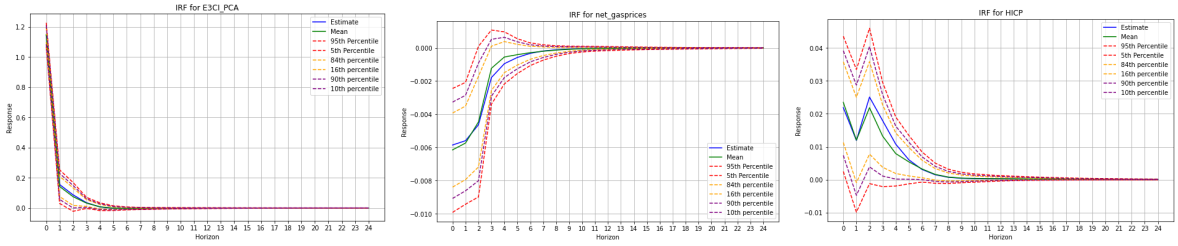

(a) E3CI PCA (b) Net price of heating gas (c) HICP excluding food and energy

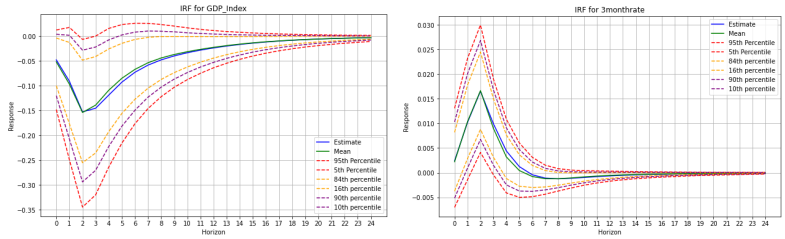

(d) GDP index (e) Three month interbank rate

Figure 7: IRFs for 5 variables using E3CI PCA and excluding HICP food and energy, 20000 bootstrap iterations

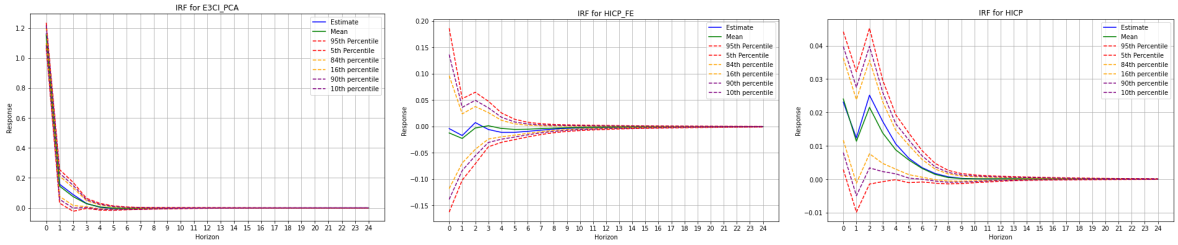

(a) E3CI PCA (b) HICP food and energy (c) HICP excluding food and energy

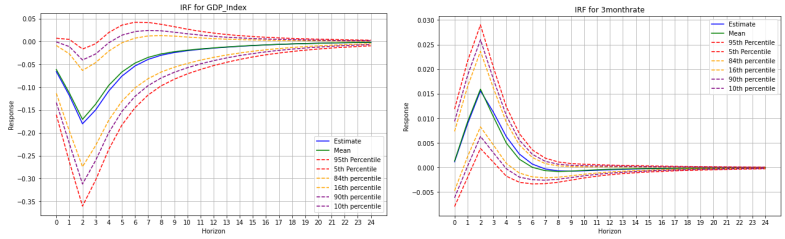

(d) GDP index (e) Three month interbank rate

Figure 8: IRFs for 5 variables using E3CI PCA and excluding net price of heating gas, 20000 bootstrap iterations

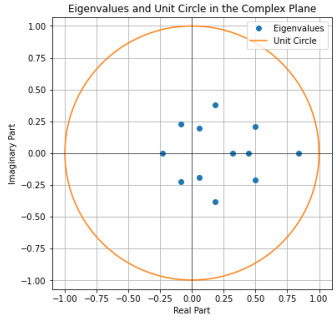

Figure 9: Unit disk and Eigenvalues for the 6 variables Var estimated using E3CI PCA

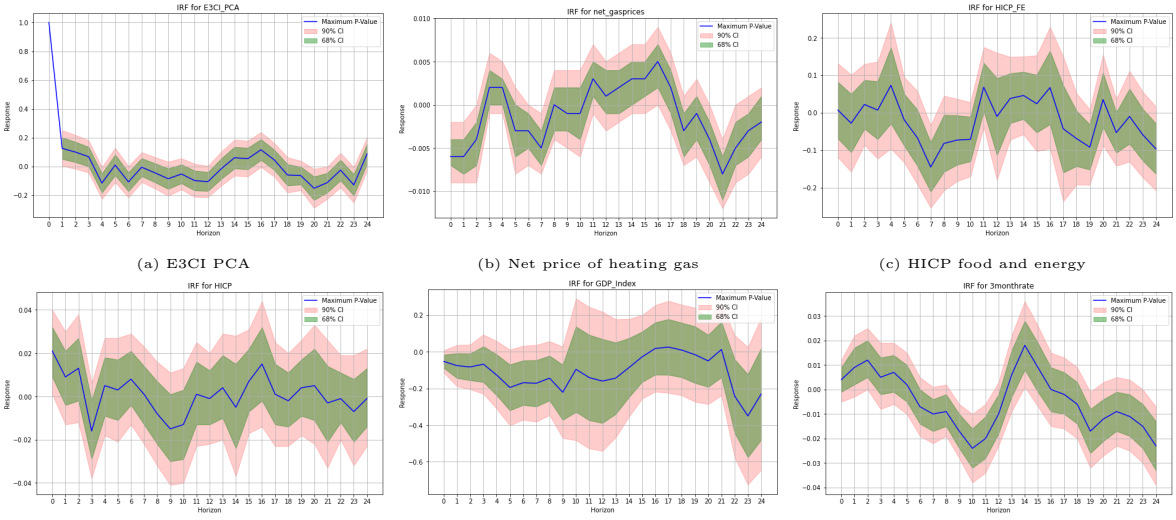

(a) E3CI PCA

(b) Net price of heating gas

(c) HICP food and energy

(d) HICP excluding food and energy

(e) GDP index

(f) Three month interbank rate

Figure 10: IRFs for 6 variables using E3CI PCA and Local projection, grid (-1,1.2) step of size 0.001